ANALYSIS OF MULTIPLE MUON RATES AND DISTRIBUTION OF MUON PAIRS DEEP UNDERGROUND

H.E. Bergeson, J.C. Boone, J.W. Elbert, G.H. Lowe, M.O. Larson and J.L. Morrison
Dept. of Physics, Univ. of Utah, Salt Lake City, Utah (USA) 84112
G.W. Mason
Dept. of Physics, Brigham Young University, Provo, Utah (USA) 84602

Multiple muon event rates measured at the Utah Muon Detector are presented for showers with 1-5 parallel muons detected in an area of 80 m^2 at depths 2.4 - 8.0×10^5 g cm^{-2} and also for high multiplicity showers with 10-30 muons detected in an area of 100 m^2 at depths 1.6 - 2.0×10^5 g cm^{-2}. Monte Carlo calculations based upon scaling and a primary spectrum and composition extrapolated from lower energies agree well with observed rates as a function of multiplicity alone, but predict a too narrow distribution of muon pairs as a function of separation (decoherence curve). Scaling up transverse momentum (x 1.5) improves agreement with the decoherence curve, but agreement with the rates is then poorer.

1. Introduction. The University of Utah underground muon detector gathered information on more than 2×10^5 muons during the course of its existence between 1968 and 1974. The events were observed under varying thicknesses of overburden in such a way as to yield information on primary cosmic rays with energies between 10^{13} and 10^{16} eV. The data are extensive enough to put rather tight restrictions on models of high energy nuclear physics as well as assumptions about primary spectrum and composition. Because of recent interest in the predictions of "scaling" and in the possible breakdown of scaling, we have developed a detailed scaling model which makes predictions of muon rates in the Utah detector.

2. Experimental. (For a description of the Utah experiment and additional references, see Lowe et al. 1975.) The present work represents one in a continuing series of analyses which have paralleled the accumulation and reduction of the muon data. The data may be grouped into three groups for purposes of discussion: 1) multiplicities 1-5 observed in an 80 m^2 fiducial area, 2) multiplicities 10-29 observed in a 100 m^2 fiducial area, and 3) distributions of separations of muons. (See Figures 1, 2, and 3.)

The data of group 1 were presented in comparison to a scaling model at the Denver Conference (Mason and Elbert 1973, Lowe et al. 1973), though they appear here with better statistics for all points. Briefly they consist of rates of events for which a given number of muons, n_D, is detected exclusively in an 80 m^2 area. The rates are accumulated as a function of zenith angle, θ, and slant depth of overburden, h. The detector was located under a rugged mountain range so that a variety of combinations of slant depth and angle were possible, but for purposes of presentation they have been centered in three angular bins (47.5, 62.5, and 72.5 degrees) and eight depth bins (2.4, 3.2, 4.0, 4.8, 5.6, 6.4, 7.2, and 8.0×10^5 g cm^{-2} standard rock).

The data of group 2 are presented here for the first time. These "supermultiple" events involve observations of ≥ 10 muons in a fiducial area of 100 m^2 at a depth of either 1.6 or 2.0×10^5 g cm^{-2} and a zenith angle of 30 degrees. These large events were not detectable until 1973 when an enlarged

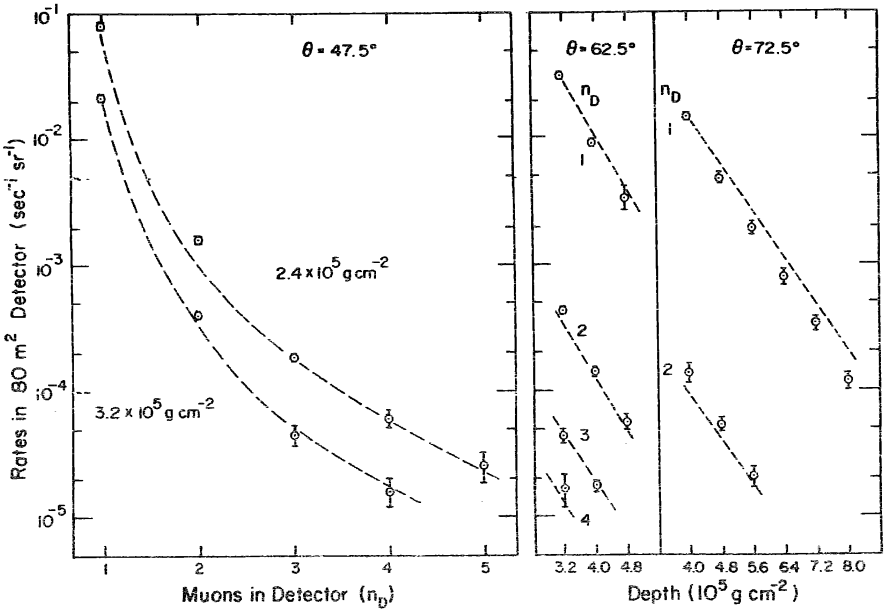

Fig. 1. Rates in an 80 m^2 detector vs. muon multiplicity and depth. The curves shown pass through the predictions of a Monte Carlo model for which the statistical uncertainties are comparable to that of the data but are not shown.

memory was installed in the data collection system to handle the increased number of spark coordinates which define the trajectories of the muons in large events. Besides making the observation of very large events possible, this improvement in the detector led to a small correction in the rate for $n_D = 5$ which is now incorporated in the data presented. The large events were sufficiently complicated to require computer programs adapted specifically to them. In particular, because of soft showers emanating from the muon tracks, muons closer together than .29 meter were considered to be one and this condition was included in the model calculations to which the data are compared. Detector triggering efficiency was greater than 99% for these events with dead time excluded. Spark counter efficiency corrections were negligible because of large counter redundancy at small zenith angles. Events which proved too difficult for the computer program were hand scanned. Scanning also showed the average muon count to be good to within 10%. The data were gathered over zenith angle range 20-40 degrees, but since no obvious zenith angle dependence could be discerned, the data were simply combined in a bin at 30 degrees. To center the data to the two depths (1.6 and 2.0×10^5 g cm^{-2}), the rates for given multiplicity were fitted to a function of depth using a maximum likelihood method based upon Poisson statistics. The resulting functions were used to yield the predictions for the specific depths chosen for display. (A similar procedure was used for the data of group 1.)

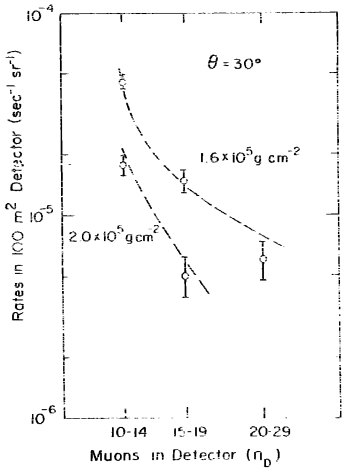

Fig. 2. Rates in a 100 m^2 detector vs. muon multiplicity.

The final group of data consists of the measured separations of muons. These separations were measured out to 60 meters using the main detector in conjunction with three portable "outriggers" deployed along a nearby tunnel. The data are organ-

ized as a decoherence curve, i.e., the rate of pairs of coincident muons in two small detectors as a function of their separation, divided by the product of the areas of the detectors. These data are discussed in more detail in an accompanying paper (Lowe et al. 1975).

3. Theoretical Model. Calculations of the expected rates depend on the nuclear physics assumed for the collision processes as well as the shape and composition of the primary spectrum. The nuclear physics of the present calculation is based on scaling (Feynman 1969). The essential features are:

1) proton-Berryllium and proton-Aluminum production cross sections at 19.2 GeV (Allaby et al. 1970) are used for an interpolation to obtain p-air cross sections. Distributions for production of protons, pions, and kaons are suitably parameterized as functions of P_T and $x = 2P_L/s^{\frac{1}{2}}$ (P_T, P_L are transverse and longitudinal momentum; s is the square of the center of mass energy). Scaling behavior is then assumed.

2) We include production of nucleons, antinucleons, pions and kaons (Elbert et al. 1975). The multiplicities of the produced particles vary asymptotically with primary energy as ln s.

3) The p-air inelastic cross section rises with energy according to:
$\sigma_{p\text{-}air} = 280 + 2.5\ \ln^{1.8}(E/100\ \text{GeV})$ mb (Yodh et al. 1972).

4) Meson-induced collisions are simulated from p-air distributions according to a prescription suggested by the quark model and supported by accelerator measurements (Elbert et al. 1971). A "leading meson" is provided.

5) The average P_T value for all pions with $x \geq 0.01$ is 0.38 GeV/c.

6) The mean inelasticity of the incident nucleon is 0.58.

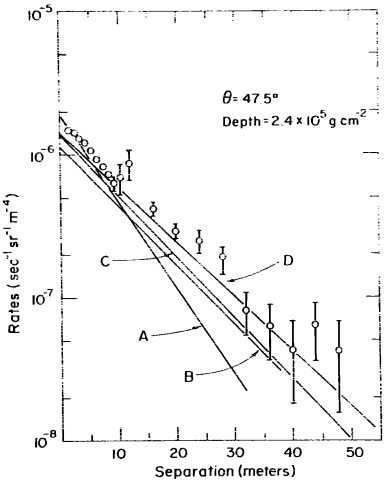

Fig. 3. Muon decoherence data. See text for description of the curves A-D.

We assume the spectral shapes of the primary components (protons, alpha particles, etc., up to and including iron) follow power laws of the form $AE^{-\gamma}$ (A will be referred to as the amplitude and γ as the spectral index). Because the present analysis is not very sensitive to the location of a "kink" or break in the primary spectrum we have used air shower results to give the approximate location (3×10^{15} eV for protons) of a rigidity dependent break in the spectrum of all primaries. Above the break the spectral index is assumed to be 3.3 (Greisen 1965).

4. Analysis. We group the primaries into three groups (protons, Z = 3-14, Z = 15-26), with the relative amounts of each element maintained within a group at values from low energy measurements (Z = 2, Ryan et al. 1972; Z = 2-9, Cartwright et al. 1971; Z = 10-28, Shapiro and Silberberg 1970; Z = 26, Balasubrahmanyan and Ormes 1973). The primary spectrum is segmented (1-2, 2-4, 4-8 . . . TeV). Monte Carlo predictions assuming spectral indices of 2.7 are made separately for each of the primary groups and each of the spectral segments. These "building blocks" can be weighted to approximate various assumptions

about the primary spectrum and composition. Previously we fitted our model to the data described above except for muon separations (Mason and Elbert 1973; Elbert et al. 1975). In doing so we found that an extrapolation of spectral and compositional parameters from below 10^{13} eV provided predictions that were in very good agreement with rates including the "supermultiples" which originate with the highest energy primaries in our experiment (~5×10^{15} eV). The best fit, with $\chi^2 = 36.5/30$ yields $\gamma = 2.75 \pm 0.02$ and $A_p = (2.3 \pm 0.2) \times 10^4$ $m^{-1}s^{-1}sr^{-1}GeV^{-1}$. In our fit the heavier components of the composition are held constant relative to the protons as a function of energy at values taken from measurements at energies ranging from 2 GeV/nucleon to 500 GeV/nucleon. The amplitude of the resulting spectrum of all primaries on a total energy basis (below the break mentioned above) is 2.5 times the amplitude, A_p, of the primary proton spectrum. The results of the fit are strikingly close to the parameters measured (Ryan et al. 1972) near 10^{12} eV. The Ryan parameters are: $\gamma = 2.75 \pm 0.03$, $A_p = (2.0 \pm 0.2)\times10^4 m^{-2}s^{-1}sr^{-1}GeV^{-1}$. In Figure 4 we show approximate relationships between primary proton energy, detected multiplicity and depth for the Ryan parameters. If the primaries are iron nuclei and energies are plotted per nucleon, the Figure is qualitatively similar but compressed to the range 10^{13}- 2×10^{14} eV/nucleon.

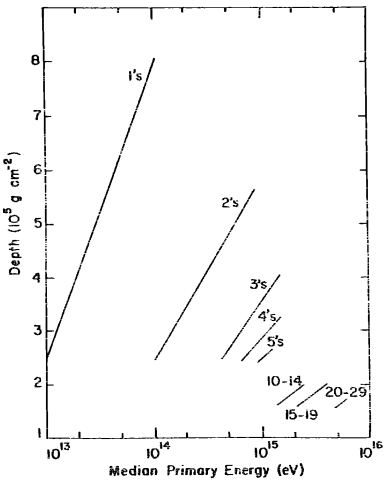

Fig. 4. Estimated relationship between primary proton energy, detected muon multiplicity and depth underground.

Recently we have compared the predictions of our model to the decoherence curve calculated from the muons. Both data and Monte Carlo calculation indicate that the decoherence curve may be roughly parameterized as an exponential, $R_0\exp(-x/x_0)$, where x is the separation of the muons. However, the model discussed above predicts an exponential falloff parameter, x_0, which is consistently smaller than that exhibited by the data. An example of this may be seen in Figure 3 where curve A represents the decoherence curve predicted by our parameters for the spectrum. It is not practical, at present, for us to include in toto the decoherence curves in our fitting procedure. Instead we have made use of the decoherence curve integrated once over area. The resulting "pair rate" is the rate of coincident pairs of muons, one of which passes through a small detector, divided by the area of that detector. For an exponential decoherence curve this is equal to $2\pi R_0 x_0^2$. We have, therefore, added as "data points" pair rates at 2.4×10^5 and 3.2×10^5 g cm^{-2} at 47.5 degrees and 3.2×10^5, 4.0×10^5 and 4.8×10^5 g cm^{-2} at 62.5 degrees to represent the decoherence curves in the fits.

Physically, the exponential falloff parameter of the decoherence curve is closely related to the transverse momentum of pions and kaons which produce the observed muons. The simplest way of bringing the decoherence curve shape into agreement with the data would be to scale up the transverse momenta in the model by a constant factor. When only this change is made, the showers spread out of a finite detector, the predicted ratios of higher multiplicities to singles decreases, and the predicted pair rates, which are independent of P_T, remain too low. We have applied a scaling factor to P_T of 1.5 which was estimated to bring about agreement with the shape of the decoherence curve. The resulting decoherence

curve is shown as curve B in Figure 3, where again the spectral parameters of curve A have been used. As expected, x_0 is much improved, but the normalization, R_0, is not as good. Most seriously affected is the ratio of doubles to single muons which decreases by as much as 40-50%. If the spectral parameters are relaxed, one can allow the overall normalization of the proton component at 1 TeV, the spectral index of the proton component, and the spectral index of the component containing iron to vary. The resulting fit yielded $\chi^2 = 85/34$. The normalization favored was 90% of the Ryan et al. (1972) value, a proton index of 2.66 and an iron index of 2.62. An example of a resulting decoherence curve is shown as C in Figure 3. This fit was used to construct the curves in Figures 1 and 2 and is the basis for Figure 5. One favorable by-product of this spectrum, as opposed to an extrapolation of the Ryan spectrum, is that when evaluated at the assumed break location at 3×10^{15} eV per particle, the all particle integral spectrum is enhanced by a factor of 1.4 to within a factor of 1-3 of that estimated from air shower measurements (Mason et al. 1975).

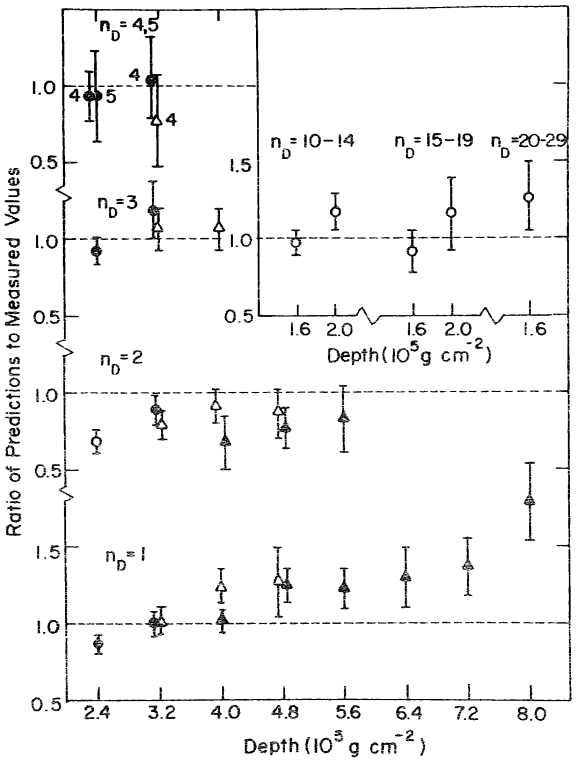

Fig. 5. Ratios of predictions to measured values for the model of curve C of Figure 3.

It has been argued that if scaling is to provide agreement with air shower development, particularly as measured at Mt. Chacaltaya, the primaries would need to be heavy, possibly iron (Gaisser 1974). Such a possibility would occur if the flatter iron spectrum observed up to 100 GeV/nucleon (Balasubrahmanyan and Ormes 1973) were to continue with a spectral index of 2 compared to protons with 2.7. Iron primaries would provide a wider muon decoherence curve than protons for the same mean P_T and primary energy because the showers develop faster producing muons at higher altitude. If we assume that iron dominates the primary spectrum at the position of the break at 3×10^{15} eV (iron break model), the break on an energy per nucleon scale occurs at about 60 TeV per nucleon. We tried a fit of the 3-parameter type tried for curve C of Figure 3 with the result that $\chi^2 = 92/34$, the overall amplitude was 87% of the Ryan et al. (1972) value, the proton index was 2.64 and the iron index was 2.55. The resulting improvement in the decoherence curve is labeled D in Figure 3. Again the fit to the doubles rate is most seriously affected.

5. Discussion and Conclusions. Underground muon data of the type obtained with the Utah muon detector can be used to place restrictions on possible assumptions about high energy nuclear physics and the cosmic ray spectrum and composition. We have used the data to test a detailed model involving scaling, a feature of which is an energy independent P_T distribution taken from accelerator measurements having a mean P_T for pion ($x \geq 0.01$) of 0.38 GeV/c. We found that the model predicts well the rates of underground muons as a function of multiplicity

and depth, but predicts a muon decoherence curve which is too narrow. The data are restrictive enough to prevent bringing about complete agreement between model and data by the simple process of scaling up the transverse momentum in the model by the constant factor of 1.5 which the decoherence data alone requires. In this latter process the rates in a finite detector of events with several muons are substantially changed in a way that cannot be corrected by acceptable changes in the assumed spectrum and composition. If the factor 1.5 is, however, approximately correct, then the data tentatively require a mean P_T for pions of ~0.6 GeV/c. This is in agreement with the conclusions of other workers who have analyzed portions of the Utah data using a CKP model (Adcock et al. 1969) and both CKP and scaling (Goned et al. 1975).

The uncertainties associated with the lateral spread of the muon showers can be avoided by selecting a part of the data. The muon pair rates add to the muon intensities additional information which can be predicted independently of the lateral structure of the muon showers. An example of such an attempt is given in Mason et al. (1975).

In view of the many uncertainties in parameters of the overall model, among which are uncertainties in the production distributions, nuclear breakup in the atmosphere, muon energy loss in rock (particularly at the larger depths) and the shape of the transverse momentum distribution as a function of energy, we view the model as largely successful in its predictions of the Utah data. It is quite possible, for example, that a changed shape of the transverse momentum dependence might improve agreement of the predicted rates while maintaining agreement with the decoherence curve, but it is clear that the data are restrictive enough that such a change cannot be arbitrary.

6. Acknowledgments. This work is supported by the National Science Foundation, Washington, D. C. (USA).

REFERENCES

Adcock, C. et al. 1970, J. Phys. A. 3 pp. 696-707.
Allaby, J. V. et al. 1970, CERN Report 70-12.
Balasubrahmanyan, V. K. and Ormes, J. F., 1973, Astrophy. J. 186, p. 109.
Cartwright, B. G. et al. 1971, Proc. 12th Int. Conf. on Cosmic Rays, Hobart vol. 1 (Hobart: University of Tasmania), pp. 215-20.
Elbert, J. W. et al. 1971, Phys. Rev. D 3, pp. 2042-7.
Elbert, J. W. et al. 1975, J. Phys. A. 8, pp. L13-17.
Feynman, R. P., 1969, Phys. Rev. Lett. 23, pp. 1415-7.
Gaisser, T. K., 1974, Nature 248, p. 122.
Goned, A. et al. 1974, preprint, University of Durham.
Greisen, K., 1965, Proc. 9th Int. Conf. on Cosmic Rays, London, vol. 2 (London: The Institute of Physics and The Physical Society), pp. 609-15.
Lowe, G. H. et al. 1973, Proc. 13 Int. Conf. on Cosmic Rays, Denver, vol. 3 (Denver: University of Denver), pp. 1878-83.
Lowe, G. H. et al. 1975, accompanying paper (MN 3-17) in these proceedings.
Mason, G. W. and Elbert, J. W., 1973, Proc. 13th Int. Conf. on Cosmic Rays, Denver, vol. 3 (Denver: University of Denver), pp. 2348-55.
Mason, G. W. et al. 1975, accompanying paper (EA 3.2-14) in these proceedings.
Ryan, M. J. et al. 1972, Phys. Rev. Lett. 28, pp. 985-8.
Shapiro, M. and Silberberg, R., 1970, Ann. Rev. Nucl. Sci. 20, p. 323.
Yodh, G. B., Pal, Y. and Trefil, J. S., 1972, Phys. Rev. Lett. 28, pp. 1005-8.